On the Structure of Glassy Polymers. VIII. Use of *Z* Contrast to Elucidate the Microstructure of Epoxy and Polyimid Resins

G. V. DI FILIPPO,* J. B. VANDER SANDE, and D. R. UHLMANN,† *Department of Materials Science and Engineering, Massachusetts Institute of Technology, Cambridge, Massachusetts 02139*

Synopsis

The technique of ultramicrotomy of polymers, followed by staining of the resulting thin sections with heavy metal ions and viewing with *Z* enhancement in the scanning transmission electron microscope is described. When applied to anhydride-cured epoxy resins, the structure is found to be heterogeneously crosslinked on a scale of a few hundred angströms. When the technique is applied to amine-cured epoxy resins, the microstructure is found to change from homogeneous to inhomogeneously crosslinked, depending on stoichiometries and cure cycles. For amine-cured resins whose cure conditions are within the range of microstructural change, the bright field of the stained specimens alone does not detect heterogeneities, and the *Z* contrast becomes crucial to discern the kind of microstructure. A commercial polyimide film examined in the same way is found to exhibit systematic variations in structure through the thickness of the film.

INTRODUCTION

Several experimental techniques have been used to detect heterogeneities, both real and artifactual, in amorphous polymers. These include small angle X-ray scattering (Ref. 1, e.g.), scanning electron microscopy (Ref. 2, e.g.), and most notably transmission electron microscopy (Refs. 2–7, e.g.). In the case of amorphous thermoplastics, the most widely used technique has been direct transmission electron microscopy of thin films cast from solution.[3,4] In the case of epoxy resins, the most widely used technique has involved two-stage replication of etched and unetched fracture surfaces and free surfaces.[2,5–7]

In all the electron microscope studies cited, evidence was found for structural heterogeneities present in large volume fractions. In the case of the glassy thermoplastics, subsequent investigations using a variety of techniques including electron microscopy and small angle X-ray scattering have indicated that the heterogeneities are not representative of the bulk polymer (see discussion in Ref. 8). In contrast, heterogeneous structures in at least some epoxy resins have been confirmed by small angle X-ray scattering (Ref. 1, e.g.).

*Current Address: Departamento de Tecnología de Materiales, INTEVEP, S.A. Apartado Postal 76343 Caracas 1070A, Venezuela.

†Current Address: Department of Materials Science and Engineering, University of Arizona, Tucson, AZ 85721.

Journal of Applied Polymer Science, Vol. 35, 485–505 (1988)
 CCC 0021-8995/88/020485-21$04.00

Other works[9] used plasma etching followed by Pt-Pd/C replication to examine the structure of glassy polystyrene and polymethyl methacrylate as well as two cured epoxy resins. A similar level of inhomogeneity (globules on the range of 200–400 Å) was found for all four materials. Since the glassy thermoplastics had been shown to be homogeneous using a variety of techniques, the last study (which is a significant one) underscored the need for an electron microscope technique which would permit structural features, if present, to be characterized with increased confidence. The issue is of particular concern for thermosetting resins such as the epoxies which undergo only a small change in density on curing.

The present paper reports such a technique and illustrates its application to elucidate the structure of epoxy and polyimide resins. The technique involves ultramicrotomy of bulk specimens to produce thin sections appropriate for electron microscopy. The thin sections are then stained using solutions of a heavy metal salt, and are viewed in the scanning transmission electron microscope in the Z contrast mode. In this mode,[10] the inelastic "bright field" and annular dark field images of the stained sample are combined to produce an image with greatly enhanced contrast.

EXPERIMENTAL

The epoxy resins and curing agents used in this study are part of those described in two companion works,[11,12] and are shown together with their corresponding cure schedules in Table I. Two types of epoxy resins were

TABLE I
Resins, Curing Agents, Cure Conditions, Preparation of the Thin Sections, Mode Employed in the STEM and Figure Number of the Corresponding Micrograph of the Materials

Sample no.	Resins and curing agent (phr)[a]		Cure conditions	Thin section	STEM[b] mode	Figure no.
1	DGEBA	(100)	1 h/RT	Stained	BF	1
	TETA	(16.6)	4 h/80°C			
2	TGEG	(100)	24 h/72°C	Unstained	BF	2(a)
	NMA	(41.6)		Unstained	BF/ADF	2(b)
	DDSA	(50)		Stained	BF	2(c)
	BDMA	(2.7)		Stained	BF/ADF	2(d)
3	TGEG	(100)	2 h/70°C	Stained	BF	3(a)
	NMA	(89)		Stained	BF/ADF	3(b)
	BDMA	(1.5)		Stained	BF/ADF	3(c)
4	DGEBA	(100)	1 h/RT	Stained	BF	4(a)
	TETA	(12)	8 h/84°C	Stained	BF/ADF	4(b)
5	DGEBA	100)	7 h/120°C	Stained	BF/ADF	5
	TETA	(12)				
6	Kapton[c] 500-H			Stained	BF/ADF	6(a)
	Film			Stained	BF/ADF	6(b)
				Stained	BF/ADF	6(c)

[a] phr = parts per hundred parts of resin by weight.

[b] Figure 1 was taken on a TEM at 40K× on plate. The magnification on plate for Figure 3(c) was 50K×. All others were taken at 200K× on plate.

[c] Commercial tradename of E. I. du Pont de Nemours and Co.

employed: (1) systems based upon the diglycidyl ether of bisphenol-A (DGEBA), whose commercial name is Epon 828 (Shell), supplied by Stephenson Chemical Co., Danbury, CT, and was cured with triethylene tetramine (TETA); and (2) systems based upon triglycidyl ether of glycerol (TGEG), Epon 812 (Shell), which was cured with nadic methyl anhydride (NMA), dodecenyl succinic anhydride (DDSA), and benzyl dimethylamine (BDMA), which was used as the accellerator of the cure. The Epon 812 and all the curing agents were supplied by Fisher Chemical Co. The mixing, casting, and cure procedures are shown elsewhere.[11,12] The polyimide investigated was a Kapton 500-H film supplied by E. I. du Pont de Nemours and Co.

Thin sections appropriate for examination in an electron microscope were obtained by ultramicrotomy of the bulk epoxy and the polyimide film. For this purpose, an LKB 4800A ultramicrotome with a diamond knife was employed. The thin sections produced in this way had nominal thicknesses of 400–600 Å. After the microtomy, the thin sections were floated on water and collected on copper grids. The staining solutions consisted of an aqueous solution of 0.7 g of uranyl acetate in 100 mL of distilled water (solution 1), and 1.0 g of uranyl acetate in 100 mL of methanol (solution 2). The copper grids containing the thin sections went through the following staining schedule: (1) rapid ($\sim$ 0.5 s) immersion of the grid in acetone, followed by immediate placement over filter paper to remove excess moisture; (2) resting the grid upon a drop of solution 1 with the sample thin section facing the solution for 15 min; (3) immersion for 10 min in solution 2. This was done in a small sealed container in order to avoid excessive evaporation of the methanol; and (4) repeat of step 1 to rinse out salt which might remain on the surface.

After staining, the samples were viewed in a Vacuum Generators scanning transmission electron microscope (STEM). Micrographs were obtained at magnifications up to 200K$\times$ on the photographic film using both bright field and Z contrast microscopy (with the exceptions of Fig. 1, which was taken on a Phillips EM-300, working in BF at a magnification of 40K$\times$ on plate and enlarged 3$\times$, and Fig. 3(C), taken on the STEM at a plate magnification of 50K$\times$). The basic mode of operation of the STEM is the following. An extremely fine probe of electrons, ideally 2–3 Å in diameter, is scanned across the specimen, which is in the form of a thin foil. Various products of the electron–specimen interaction are then collected and used for image formation or microanalysis. The electrons which have passed through the sample and have either been forward-scattered with no change in energy or direction (inelastically scattered) or elastically scattered, can be collected by some type of electron detector and used to modulate the intensity of a cathode-ray tube, forming an image of the internal structure of the material.

The electron beam thus produced is then accelerated to a maximum of 100 kV potential. Two electromagnetic lenses demagnify the electron source to a final probe diameter as small as 3 Å at the specimen, and a set of double deflection electromagnetic coils scan this probe orthogonally across the specimen. An annular detector is situated to collect the electrons scattered through angles 0.02 rad $\leq \theta \leq$ 0.2 rad, while the forward-scattered and inelastically scattered electrons pass through the center of this detector. These electrons are collected by the electron spectrometer-bright-field detector assembly at the top of the instrument. The spectrometer allows electrons of a selected energy to pass into the bright-field detector, which produces an image com-

parable to the bright-field image in TEM (when "unscattered" zero-loss electrons are detected). The annular detector in the STEM collects the bulk of the elastically scattered electrons. Since the annular detector is nearly 100% efficient in collecting elastically scattered electrons, compared with conventional TEM, dark-field images can be obtained with a minimum electron dose, especially when the beam scanning is carefully controlled. In addition, for the annular detector the contrast mechanisms which are more important in polymeric materials are maximized, i.e., thickness contrast and atomic-number contrast.

In the Z contrast mode, both inelastic "bright-field" and annular dark field images were obtained and combined electronically to produce an image with greatly enhanced contrast between the structural features. For details on this technique, the reader is referred to Ref. 10. However, because of the importance of this imaging technique for the interpretation of the images presented in this paper, a brief description is offered below.

Consider a thin polymer film where one phase, or one class of microstructural feature, has been lightly stained with a heavy element such as U or Os. If a total N electrons is incident on the specimen, then N_e electrons will be elastically scattered, N_{in} will be inelastically scattered and $N_0 = (N - N_e - N_{\text{in}})$ will be unaffected by the specimen. Theoretical scattering cross-section calculations yield, for a thin sample,

$$\frac{N_e}{N} = \frac{46.5Z^{4/3}}{\sigma_b \cdot V} n = \frac{n\sigma_e}{\sigma_b} \tag{1}$$

$$\frac{N_{\text{in}}}{N} = \frac{868Z^{1/3}}{\sigma_b \cdot V} = \frac{n\sigma_{\text{in}}}{\sigma_b} \tag{2}$$

where Z is the atomic number, V is the accelerating potential, σ_b is the cross-sectional area of the electron beam, and n is the number of atoms being irradiated by the beam. In addition, σ_e and σ_{in} are the elastic and inelastic scattering cross sections, respectively.

Elastic scattering occurs at large scattering angles (50–100 mrad) compared to the convergence angle of the illumination ($\sim$ 20 mrad), so that most elastically scattered electrons are scattered outside the cone of illumination. The inelastic scattering process, however, is such that the angles of scattering are small ($\sim$ 1 mrad), and most inelastically scattered electrons stay within the illumination cone. Since the annular detector in the VG STEM subtends several hundred milliradians while the hole in that detector subtends 20 mrad or less, the annular detector measures predominantly N_e.

The electrons that pass through the hole in the detector can be separated into the two components N_e and N_{in} by means of the electron spectrometer. From eqs. (1) and (2) above, $N_e/N_{\text{in}} \simeq Z/19$, a relationship which is independent of specimen thickness and V to a first approximation.

Consider a simplified model for a polymer where the polymer consist of carbon (C) atoms only, in which a "second phase" exists which can be lightly "stained" with a few uranium (U) atoms. Assume that in the second phase one

out of every 100 atoms is U, i.e., $n_U/n_C = 0.01$. Then for the second phase

$$\frac{N_e^{C+U}}{N} = \frac{n_U\sigma_e^U + n_C\sigma_e^C}{\sigma_b} \tag{3}$$

and for the matrix

$$\frac{N_e^C}{N} = \frac{n_C\sigma_e^C}{\sigma_b} \tag{4}$$

and, for the second phase,

$$\frac{N_{in}^{C+U}}{N} = \frac{n_U\sigma_{in}^U + n_C\sigma_{in}^C}{\sigma_b} \tag{5}$$

for the matrix

$$\frac{N_{in}^C}{N} = \frac{n_C\sigma_{in}^C}{\sigma_b} \tag{6}$$

where n_C is the number of carbon atoms in the beam and n_U is the number of uranium atoms in the beam.

Now, for a divided image, the second phase has

$$\frac{N_e^{C+U}}{N_{in}^{C+U}} = \frac{n_U\sigma_e^U + n_C\sigma_e^C}{n_U\sigma_{in}^U + n_C\sigma_{in}^C} \tag{7}$$

while for the matrix

$$\frac{N_e^C}{N_{in}^C} = \frac{\sigma_e^C}{\sigma_{in}^C} \tag{8}$$

and using the definition of contrast

$$\frac{\Delta I}{I} = \left(\frac{N_e^{C+U}}{N_{in}^{C+U}} - \frac{N_e^C}{N_{in}^C}\right) \Bigg/ \frac{N_e^C}{N_{in}^C} = \frac{N_e^{C+U}}{N_{in}^{C+U}} \frac{N_{in}^C}{N_e^C} - 1 \tag{9}$$

Therefore,

$$\frac{\Delta I}{I} = \frac{n_U\sigma_e^U + n_C\sigma_e^C}{n_U\sigma_{in}^U + n_C\sigma_{in}^C} \cdot \frac{\sigma_{in}^C}{\sigma_e^C} - 1 \tag{10}$$

and, making the substitution $n_U = .01n_C$,

$$\Delta I/I = 0.35 = 35\% \tag{11}$$

This is far in excess of the 5–10% considered necessary for visibility. Thus,

divided images of the type described above for very lightly stained polymers will yield contrasting images capable of elucidating fine details in polymer microstructures.

RESULTS

Development of Staining Procedure

Our initial experiments were dedicated to finding a suitable staining procedure for inhomogeneous networks. The rationale for this was as follows: If a heavy, electron dense material could be "slipped" into the network structure, partitioning differently among domains of different crosslink density, a sufficient difference in electron density among differently crosslinked regions could be produced to permit their observation in the electron microscope. The staining can be effected using either an electron-dense swelling agent[13] or a solution of a heavy-metal salt. Because of the ultra-high vacuums in the column of the electron microscope, the first option was discarded (the high vapor pressures of liquid solvents would lead to total evaporation). Adopting the second option, water solutions of uranyl acetate were used. Since water is a good swelling agent for epoxy resins, the solution was expected to penetrate the network, and subsequent evaporation of the water would leave the salt within the structure. Regions with different crosslink density should take up different amounts of the heavy metal, and hence differential contrast would be generated between regions of different crosslink density.

Such contrast would represent a "negative" of the resin microstructure, since the lightly crosslinked regions will be swollen to a greater extent than the highly crosslinked ones, and thus will take up a higher amount of heavy metal salt and hence appear more opaque in TEM observations.

The initial work on staining was performed using only water solutions of uranyl acetate. This was done on a DGEBA-resin with 16 parts per hundred (phr) TETA, cured for 1 h at RT and 4 h at 80°C (sample 1, Table I). The staining time was 1 h. Bright-field TEM observations of the stained thin sections revealed white-cloudy regions, with a dispersion of sizes ranging from 200 to 800 Å, embedded in a darker background (Fig. 1). Some black spots on the surface of the thin section, due to residual uranyl salt, were also observed. It must be pointed that, although the larger inhomogeneities of sample 1, have a size comparable to the thickness of the thin section, they are interconnected together through regions with a smaller crosslink density, which get more swelling agent and hence a larger amount of electron-dense salt.

Staining times longer than 30 min did not produce any further changes in the contrast, while significantly shorter times (5 min) produced a weaker contrast. The staining time was related to the time to reach swelling equilibrium. Samples with curing times up to 40 h were highly crosslinked (see Ref. 12) and reached this equilibrium only after 1 h.

A key finding for improved staining was that "dry" thin sections (1 h in a vacuum oven at 50°C, $\sim 10^{-2}$ torr) absorbed more stain than those simply floated in water after the ultrasectioning (which were obviously swollen by pure water). The staining of the dry sample occurred by solvent swelling,

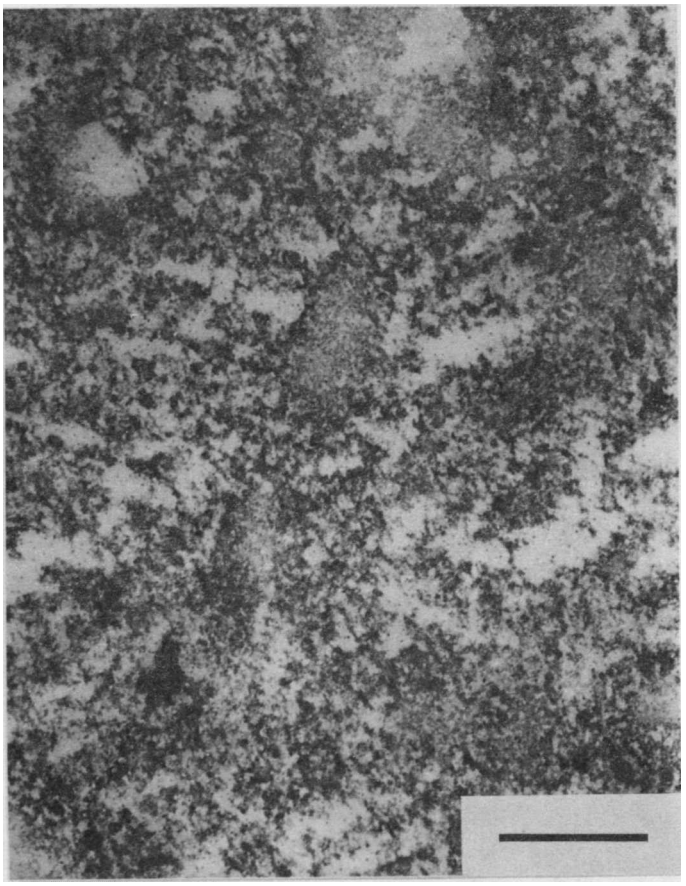

Fig. 1. 80K× BF, TEM micrograph of stained amine-cured DGEBA resin. Bar = 0.25 μm.

while that of the already-wet samples occurred by the osmotic-pressure gradient between the water and the salt solution (which is slower).

Quick immersion (~ 0.5 s) in acetone of the grid containing the thin sample, step (1) of the staining procedure, reduced appreciably the staining-equilibrium times (from 1 h, to less than 10 min) for the highly cured samples and from 30 min to approx. 5 min for the less-cured samples (e.g., sample 4 of Table I). A "safe" staining time of 15 min in step (2) was therefore used for all samples. The inclusion of step (1) did not produce any change in either the shape, size, or contrast of the inhomogeneities observed for a given sample.

When some amino formulations produced featureless resins in BF mode (e.g., samples 4 and 5 in Table I), a step including a better swelling agent than water was included: methanol solutions of uranyl acetate (solution 2) were included in the procedure as step (3). Inclusion of this step did not reveal any inhomogeneities in the featureless resins [even when the times in steps (2) and (3) were increased up to 1 h each], but produced improved contrast in the resins previously found as heterogeneously crosslinked. Step (3) was found to be particularly important to reach a good staining contrast of polyimide films.[14]

The black spots on the surfaces of the thin samples were largely or completely eliminated by a quick-rinse step (~ 0.5 s) in acetone (step (4)), following the 10 min treatment with the methanol solution. This last step was first tried with distilled water; but acetone worked better for the removal of the superficial salt, and, since it did not produce any change in the shape, size, or contrast of the inhomogeneities observed for a given sample, it was maintained in the procedure.

Some sporadic superficial black spots were observed in nearly all samples, but since they were helpful in focusing the STEM (mainly in homogeneous specimens) and since they are easily identifiable and their presence did not affect the interpretation of the micrographs, more extensive washing procedures for their removal were not attempted.

This sequence of observations led to the development of the four-step staining procedure outlined above. The procedure proved to be highly reliable and provided experimental results with a high degree of reproducibility. It was used for all the resins presented in Table I.

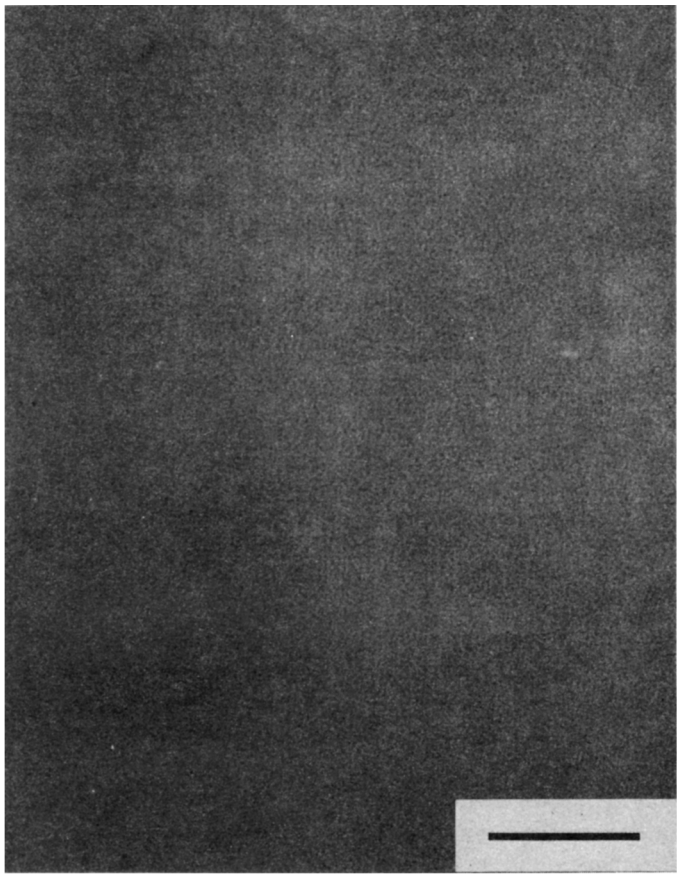

(a)

Fig. 2. 200K× STEM micrographs of anhydride-cured TGEG resin: (a) unstained BF; (b) unstained BF/ADF; (c) stained BF; (d) stained BF/ADF. Bar = 0.1 μm.

No attempt was made to describe the staining in terms of chemical reactions, since the short times necessary for obtaining good staining and the low temperature (RT) at which the procedure was carried out did not provide the conditions for such reactions. At high temperatures (above 60°C at least), reactions could occur either by carboxylate substitution of the acetate anion in the uranyl salt or by interaction of the uranyl cation with groups having a slight basic character (e.g., unreacted epoxides or amino groups) due to the Lewis-acid character of the cation.[15] The last reaction requires elevated temperatures; and the higher content of amino groups (bases) in the amino cured systems should render them easier to stain than the anhydride-cured resins (the polyimides cannot be compared since they contain both acid groups and amino groups). In fact, the anhydride-cured resins[12] (some of which are shown here as samples 2 and 3 in Table I) as well as the polyimides always showed higher contrast upon staining than the amine cured systems. This can be observed by comparing Figures 4(b) and 2(d).

Although the lower contrast in amine-cured systems could be due to a smaller difference in crosslink density ($\Delta\nu$) between differently crosslinked

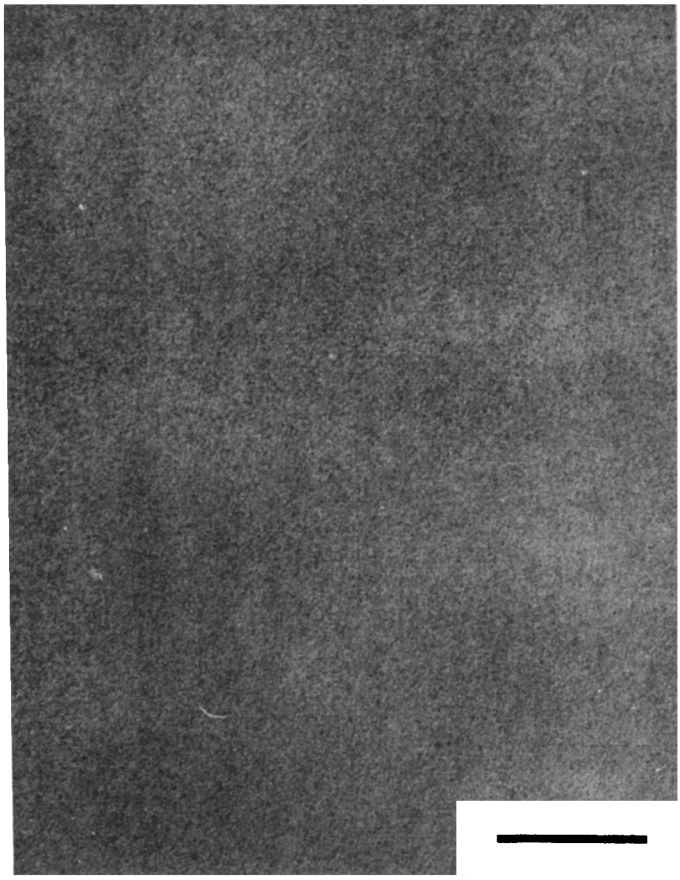

(b)

Fig. 2. (*Continued from the previous page.*)

regions, it is well established that both the anhydride-cured resins and the polyimides contain unreacted-carboxylic acid groups which could compete with the acetate group for the uranyl ion. The fully formed polyimide group is not hydrolyzable, but the polymerization reaction that leads to its formation has an acid group as an intermediate and also produces water. The anhydride-cured resins also present carboxylic-acid groups which can remain partially unreacted and hence substitute the acetate group (solvating effect) on the salt.

It is also known that the cure of epoxies by acid anhydride produces easily hydrolyzable ester groups. The hydrolysis of those groups, however, must be either acid or base-catalyzed; and, as mentioned before, the low temperature and short times used in the staining procedure, together with the almost neutral pH of the uranyl acetate solutions, strongly preclude any possibility of chemical reactions. The higher ease of staining of anhydride-cured epoxies and polyimides compared with the amine-cured systems can be explained solely on the basis of their higher hydrophylicity, due to the higher oxygen content (~ 50 wt % of anhydride components) of the mixtures undergoing cure.

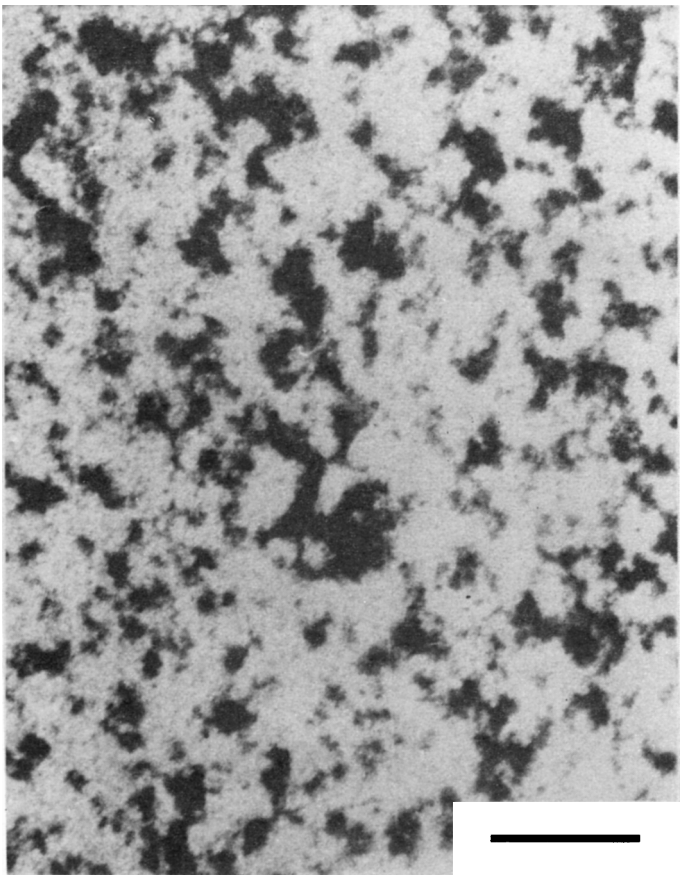

(c)

Fig. 2. (*Continued from the previous page.*)

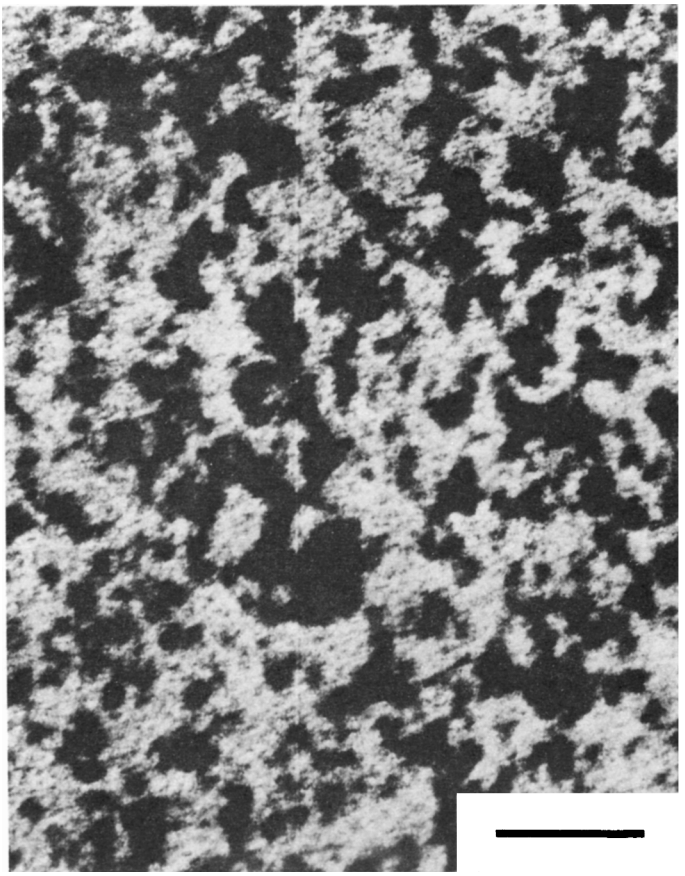

(d)

Fig. 2. (*Continued from the previous page.*)

Z-Contrast Electron Microscopy

Z-contrast microscopy[10] was carried out in the VG-STEM by combining electronically the inelastic (bright field) image with the image generated from the elastically scattered electrons (annular dark field). Since both scattering modes (inelastic and elastic) contain simultaneous contrast information from the same region of the sample but arise from partially independent sources, both contrasts are electronically added to produce an image with greatly enhanced contrast. This technique was detailed in Experimental.

The effects of the staining and the *Z*-contrast technique can be observed by its result in a representative sample, the heterogeneous anhydride-cured Epon 812 (sample 2, Table I). The bright field image did not reveal the heterogeneities [Fig. 2(a)]; the corresponding micrograph taken by the electronically divided image (BF/ADF, without previous staining) showed an increased overall darkness but did not make evident the inhomogeneous microstructure [Fig. 2(b)]. The specimen observed in Figures 2(a) and 2(b) does not show any heterogeneities since there is not enough contrast (electron-density difference)

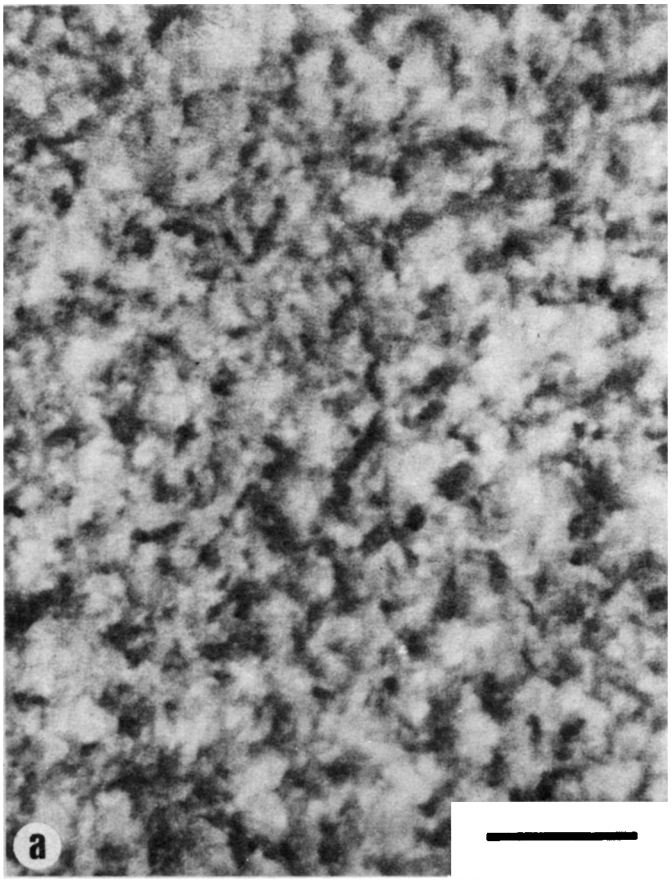

Fig. 3. STEM micrographs of anhydride-cured TGEG resin: (a) stained BF, 200K×; (b) stained BF/ADF, 200K×; (c) stained BF/ADF, 50K×. Bar = 0.1 μm for (a) and (b). Bar = 0.4 μm for (c).

between the regions of high and low crosslink density for them to be observed. The staining, besides making the thin specimens electron-conductive, thus adding stability for TEM examination and eliminating the need of C-coating (specimen drift under the electron beam was not observed for stained materials), revealed that this material was in fact heterogeneous [Fig. 2(c)]. The *Z*-contrast image of the same region of the stained material presented enhanced contrast with increased microstructural detail [Fig. 2(d)].

An analogous results is given for another Epon 812 anhydride-cured resin (sample 3 in Table I). The bright field (BF) and divided (BF/ADF) images for the unstained resin looked featureless, similar to Figures 2(a) and 2(b), respectively.

The BF image of the stained sample [Fig. 3(a)] showed again less gradation of contrast than its *Z*-contrast analogue, Figure 3(b). Figure 3(c) is a micrograph of a 50K× (magnification on plate) obtained by *Z*-contrast of sample 3 and is presented here to show an overall view of the region where Figures 3(a) and 3(b) were taken. Notice in this micrograph the "cheesy" heterogeneous morphology of this material. It is convenient to say that, because of the scan

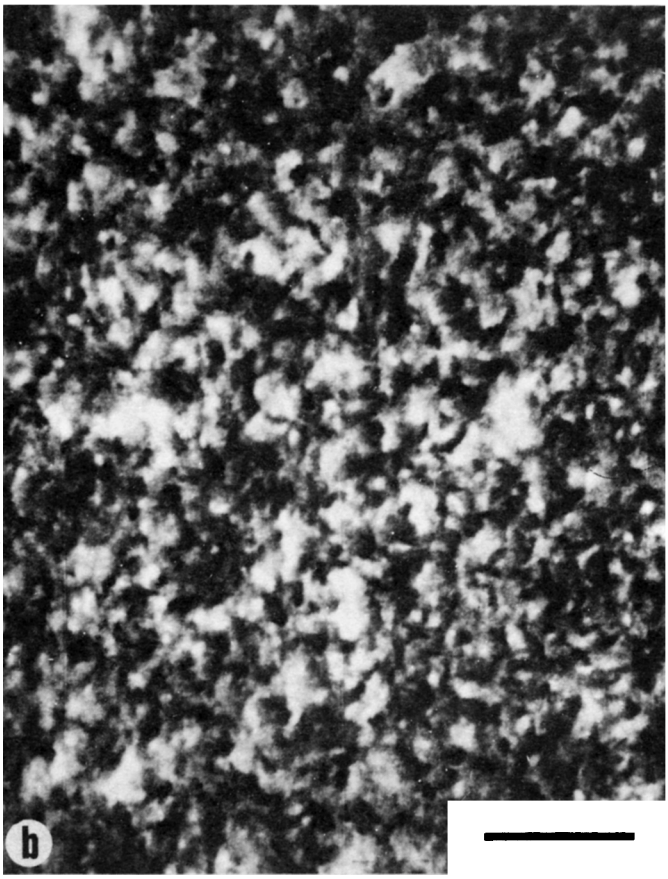

Fig. 3. (*Continued from the previous page.*)

mode of the STEM, a low electron dose is needed to record a micrograph of the microstructure of the material. Exposition times were short (3–4 s); this, combined with the increased electron-conductive capacity of the stained specimens, yielded no signs of beam damage on the materials studied; this was true even for magnifications up to 500K× on plate. Freshly exposed regions showed the same morphological details than long-time exposed ones (~ 3 min). This is probably due to the fact that, once the staining salt is trapped within a domain, there is no chance for diffusion through the solid sample. Our experience with HDPE showed that, although at magnifications of 200K×, it takes about 8 s, for the crystalline *e*-diffraction pattern to disappear, the stained domains still persist within the sample.[16]

All the anhydride-cured epoxies studied,[12,14] some of which are presented here, appeared to be heterogeneously crosslinked when the BF images of the stained specimens were observed in the STEM (see Figs. 2(c) and 3(a) for samples 2 and 3 of Table I, respectively), and the effect of the *Z*-contrast technique was to enhance the image-contrast with added structural detail; this can be observed by comparing Figures 2(c) and 3(a) with Figures 2(d) and 3(b), respectively. The same was true for stained specimens of amine-cured epoxy resins in which the amino component was in large stoichiometric excess,

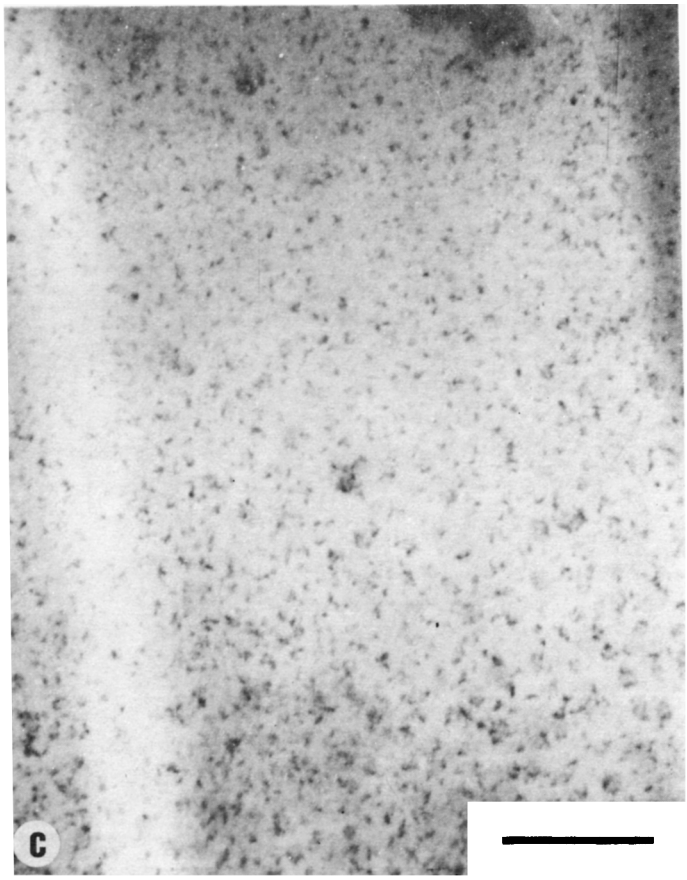

Fig. 3. (*Continued from the previous page.*)

as seen in Figure 1, corresponding to sample 1. Stereo pairs of Z-enhanced micrographs of the stained sample revealed cloudlike structures, corresponding to the highly crosslinked regions, embedded in a less crosslinked matrix. Such structural features were observed to extend throughout the entire thickness of the thin section and all over the bulk ($3D$) of the material. The latter finding was obtained by comparing the structural features observed in thin sections microtomed from different locations within the sample.

No significant variation in the observed microstructure was found when the overall staining procedure was repeated twice on a particular sample, or when the staining times in steps 2 and 3 (see Experimental above) were increased up to 1 h each. The staining conditions detailed in Experimental were therefore taken as standard for epoxy resins, and have provided useful results for the study of the development of the microstructure during the curing process of a variety of epoxy resins, both amine- and anhydride-cured, and for a wide range of temperature and times of curing. Systematic results of such studies are presented in Refs. 11 and 12, respectively.

Use of the Z-contrast mode became crucial for the investigation of DGEBA/TETA compositions close to the stoichiometric amounts of re-

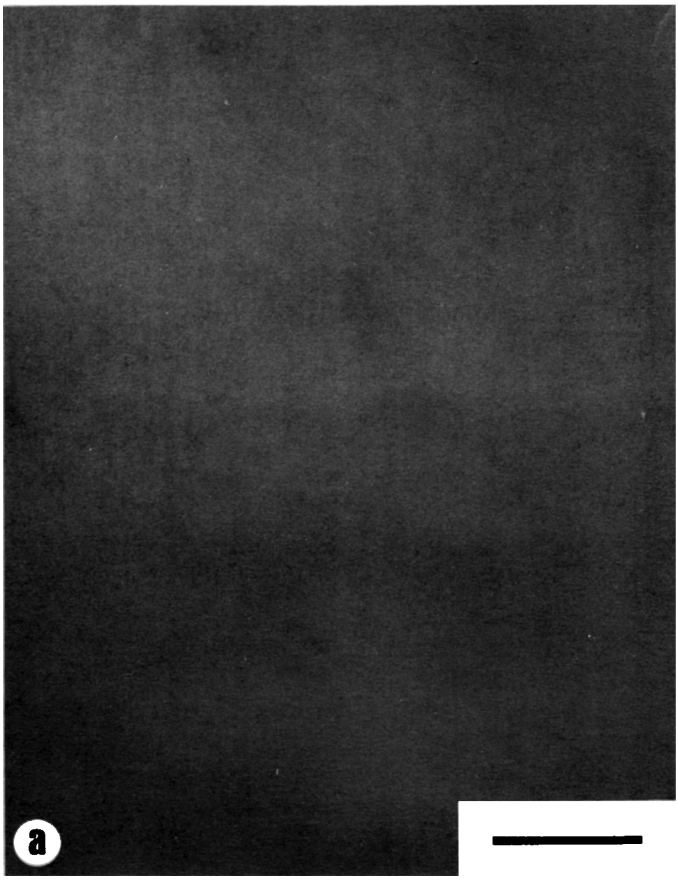

Fig. 4. 200K× STEM micrographs of amine-cured DGEBA resin: (a) stained BF; (b) stained BF/ADF. Bar = 0.1 μm.

actants (e.g., samples 4 and 5 in Table I). Of those samples, sample 5 was found to be homogeneously crosslinked, even by means of Z contrast (Fig. 5) while sample 4 was found to be heterogeneously crosslinked, but the corresponding BF image of its stained thin section was featureless. Figure 4(a) is a BF image of the stained sample 4. Although the highest contrast available in BF was utilized for obtaining this micrograph, the inhomogeneities were not apparent. When the Z-contrast mode was used, however, the inhomogeneous microstructure became visible [see Fig. 4(b)].

Similar results (heterogeneities only observable by Z-contrast) were obtained for all the TETA compositions close to the stoichiometric amounts: Depending upon slight variations in the cure cycle or composition, these samples had either inhomogeneous or homogeneous microstructures observable in the Z-contrast mode.[11] For such reasons, heavy metal staining combined with Z-contrast became a routine technique, for the investigation of the microstructure of the cured epoxy resins.

When the same staining conditions were applied to a polyimide resin (du Pont's Kapton film), useful results were also obtained. These are illustrated by the Z-enhanced micrographs of stained thin sections shown in

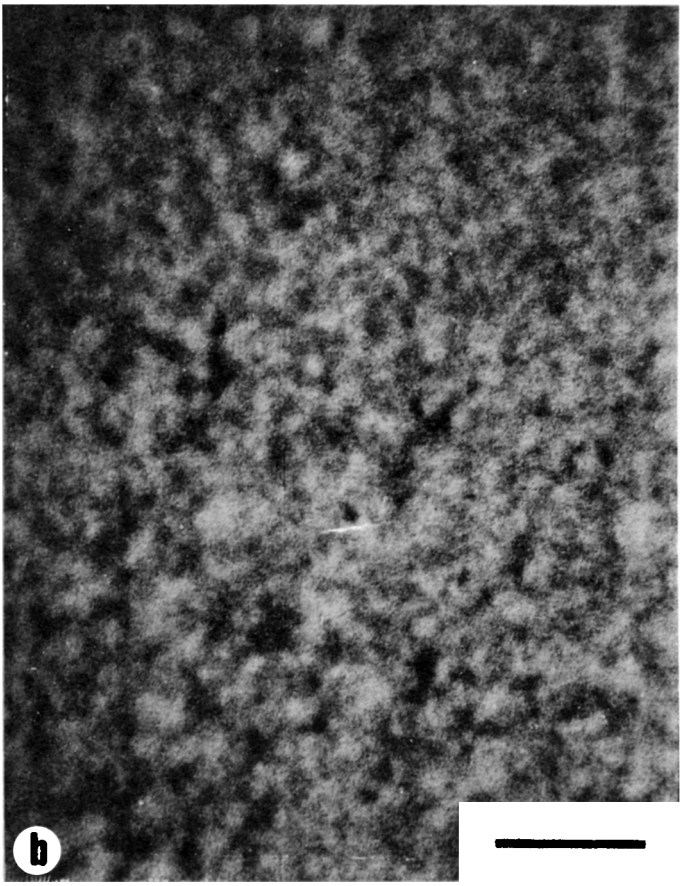

Fig. 4. (*Continued from the previous page.*)

Figure 6. The micrographs show the structures seen at different locations through the thickness of the film, with Figure 6(a) representing the structural features near one surface; Figure 6(b), the structure in the central region, and Figure 6(c), the structure near the other surface. A heterogeneous microstructure is clearly seen at all elevations through the film, with the scale and perhaps even the form of the heterogeneities varying gradually with distance from one surface to the other.

The observed variation in structure very likely reflects details of the one-step polymerization-casting process used in the manufacture of the film,[17] and no extensive explanation can be provided due to the lack of availability of the details of the manufacture process.

DISCUSSION

The combination of staining thin sections with heavy metal salts and viewing with Z enhancement in the scanning transmission electron microscope seems to provide the capability of characterizing with confidence the structural features of polymeric materials. As used in the present study, with

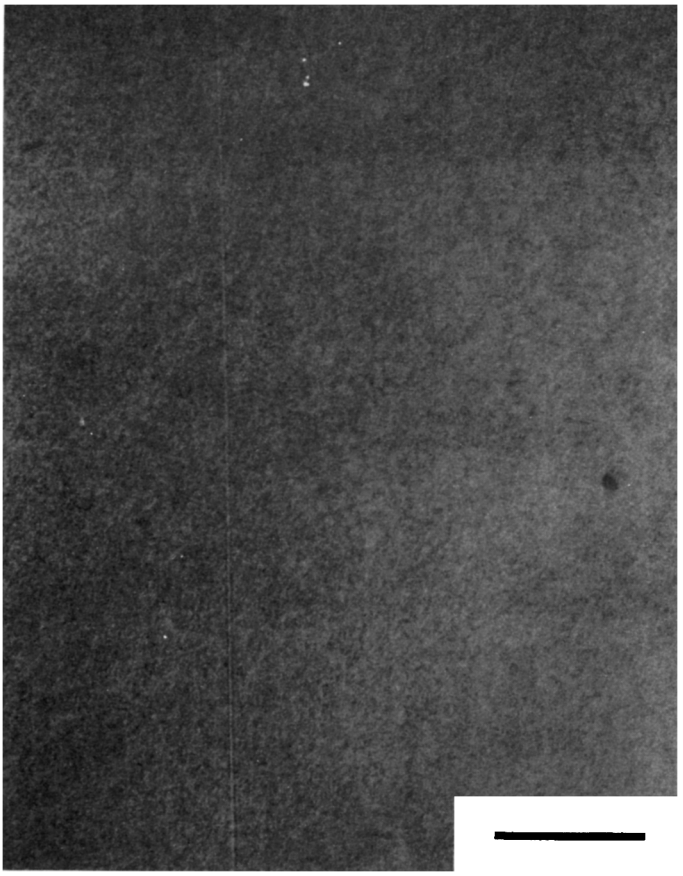

Fig. 5. 200K× STEM micrograph of amine-cured DGEBA resin. Stained BF/ADF. Bar = 0.1 μm.

uranyl acetate staining, it has been possible to elucidate the structure of both epoxy and polyimide resins with a clarity that is not possible using transmission electron microscopy of unstained samples and with a confidence that is usually not possible using replication electron microscopy.

Since the technique employs microtomed sections, it offers the possibility of characterizing the structure of bulk polymers. Based on experience in our laboratory, the process of ultramicrotomy requires considerable care to avoid introducing artifacts (chatter marks, crazing, etc.) in the thin sections; but once mastered, the technique can be used routinely and efficiently. Use of the heavy metal stain not only provides increased contrast for viewing structural features, it also provides increased permanence to the features on viewing in the electron microscope. That is, while short-range molecular rearrangements induced by the electron irradiation can wipe out structural features such as crystals at modest radiation doses, relatively long-range diffusion of the stain is required to wipe out the perception of the structural features in stained polymers; and this requires substantially higher radiation doses. Further, the use of a dedicated scanning transmission electron microscope makes it possible to record images with minimal exposure to the electron irradiation.[18]

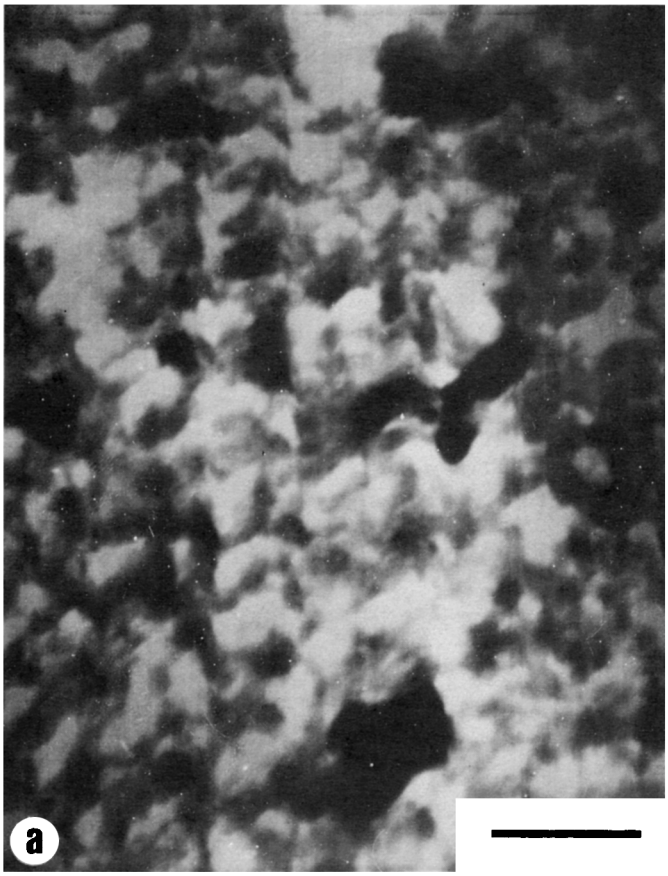

Fig. 6. 200K× STEM micrographs of stained Kapton polyimide film: (a) region near one surface; (b) central region of film; (c) region near other surface. Bar = 0.1 μm.

A variety of carrier solvents can be used with the heavy metal stain to effect its penetration into the thin section. The water and methanol used in the present investigation were found to provide good results for the polymers studied. With an appropriate carrier, the heavy metal ions (uranyl ions in the present case) will diffuse into the thin section, and will be concentrated in the less crosslinked-phase which will then appear dark in micrographs such as Figure 3(b). As mentioned before, because of the Lewis-acid character of the uranyl cation,[15] the potentiality of it interacting with unreacted epoxy groups, or with the curing agent cannot be discarded and is presently under study. In work to be reported elsewhere,[11] it has been found possible to follow the development of microstructure through the curing of amine-cured epoxy resins. Such observations, together with the variation of structure through the thickness of a polyimide film shown in Figure 6, which may be due to the quick one-step polymerization film casting process used in their manufacture,[17] lend confidence to the use of the technique for characterizing structure even in cases where there is only a small difference in properties between specific structural features and matrix material. It must be mentioned also that when

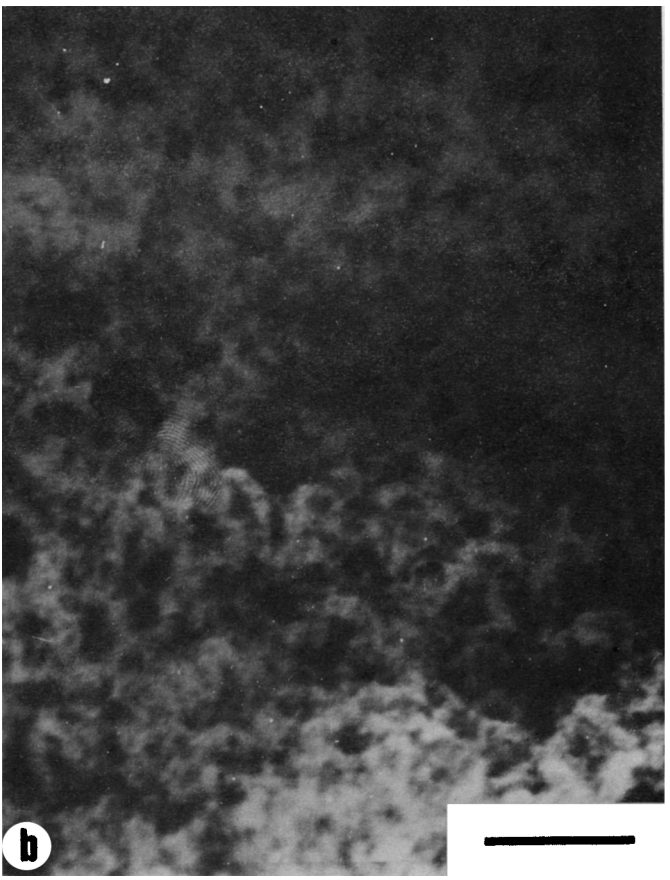

Fig. 6. (*Continued from the previous page.*)

the techniques described in the present paper were employed in standard-cured phenolic resins (resoles and novolacs), microstructural inhomogeneities of larger sizes than the reported here (~ 900 Å) present in large volume fractions were observed.[14]

In this light, it is noteworthy that examination of several glassy thermoplastics [polycarbonate, poly(ethylene terephthalate), polystyrene, and poly(vinyl chloride)] using the same technique of staining with uranyl acetate and viewing with Z enhancement revealed featureless microstructures, with no heterogeneities observable in significant volume fractions.[8]

In summary, the technique of ultramicrotomy, staining with heavy metal ions and viewing with Z enhancement seems to provide an almost-unique capability for determining the structure of polymers. In its present application, structural heterogeneities on a scale of a few hundred Å have been noted in some cured epoxy resins while others have been shown to be homogeneous. Structures on a similar scale, varying systematically through the thickness, have been observed in a polyimide film. The elucidation of such structural features and their dependence on process history should be a fruitful area of future investigation.

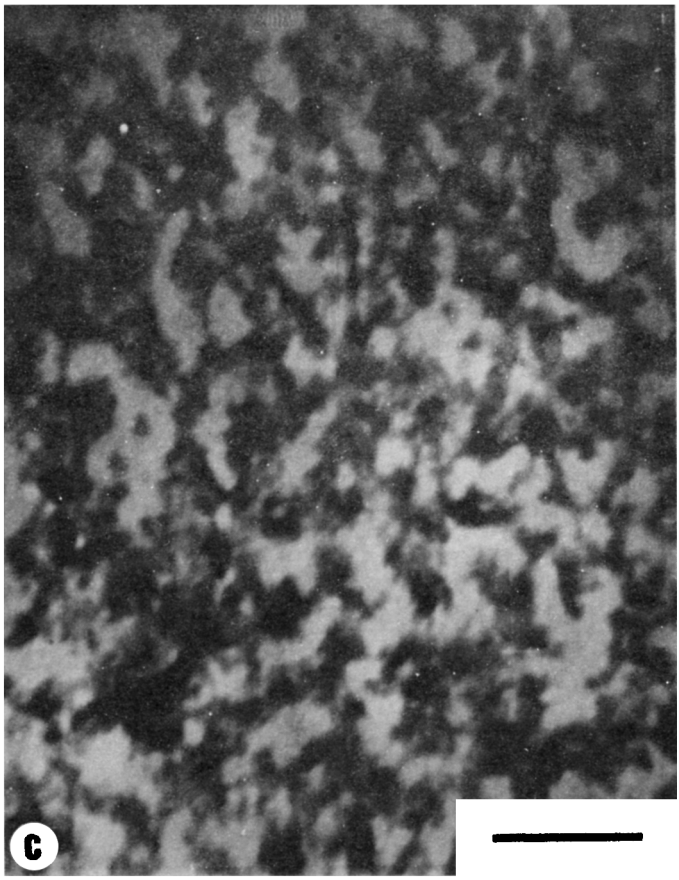

Fig. 6. (*Continued from the previous page.*)

Financial support for the present work was provided by the Air Force Office of Scientific Research. This support is gratefully acknowledged.

References

1. R. J. Matyi, D. R. Uhlmann, and J. A. Koutsky, *J. Polym. Sci., Polym. Phys. Ed.*, **18**, 1053 (1980).
2. R. J. Morgan and J. E. O'Neal, *Polym. Plast. Technol. Eng.*, **10**, 49 (1978).
3. G. S. Yeh and P. H. Geil, *J. Macromol. Sci. Phys.*, **B1**, 235 (1967).
4. J. J. Klement and P. H. Geil, *J. Macromol. Sci. Phys.*, **B6**, 31 (1972).
5. J. L. Racich and J. A. Koutsky, *J. Appl. Polym. Sci.*, **20**, 2111 (1976).
6. R. J. Morgan and J. E. O'Neal, *J. Appl. Polym. Sci.*, **23**, 2711 (1979).
7. J. Mijovic and J. A. Koutsky, *Polymer*, **20**, 1095 (1979).
8. G. V. Di Filippo, J. B. Vander Sande, and D. R. Uhlmann, *J. Appl. Polym. Sci.*, to appear.
9. K. Dusek, J. Plestil, F. Lednicky, and S. Lunak, *Polymer*, **19**, 393 (1978).
10. A. V. Crewe, J. Wall, and L. M. Welter, *J. Appl. Phys.*, **39**, 5861 (1968).
11. G. V. Di Filippo, J. B. Vander Sande, and D. R. Uhlmann, to appear.
12. G. V. Di Filippo, J. B. Vander Sande, and D. R. Uhlmann, to appear.
13. K. Dusek and J. Spevacek, *Polymer*, **21**, 750 (1981).

14. G. V. Di Filippo, Ph. D. Thesis, Massachusetts Institute of Technology, Cambridge, MA, May 1983.

15. R. V. Subramanian and M. Anand, in *A.C.S. Symposium on Chemistry and Properties of Crosslinked Polymers*, Academic, New York, 1977.

16. D. R. Uhlmann, G. V. Di Filippo, and J. B. Vander Sande, unpublished results.

17. A. L. Endrey, U.S. Pats. 3,179,630 (1965) and 3,410,826 (1968); W. M. Edwards, U.S. Pats. 3,179,614 (1965) and 3,179,634 (1965); C. E. Sroog, *J. Polym. Sci., Macromol. Rev.*, **11**, 161–208 (1976).

18. D. R. Uhlmann, Air Force Office of Scientific Research, Final Report. Grant No. AFOSR 77-3266, June 1981.

Received March 5, 1987
Accepted March 16, 1987